

# First Principles Study in the Electronic Structures and Optical Properties of Chalcogenide-doped AgInS<sub>2</sub>

Worasak Sukkabot (✉ [w.sukkabot@gmail.com](mailto:w.sukkabot@gmail.com))

Ubon Rajathanee University

---

## Original Research

**Keywords:** electronic structures, optical properties, AgInS<sub>2</sub>, density functional calculations

**Posted Date:** February 5th, 2021

**DOI:** <https://doi.org/10.21203/rs.3.rs-175295/v1>

**License:** © ⓘ This work is licensed under a Creative Commons Attribution 4.0 International License.

[Read Full License](#)

---

**Version of Record:** A version of this preprint was published at Optical and Quantum Electronics on July 22nd, 2021. See the published version at <https://doi.org/10.1007/s11082-021-03115-3>.

# Abstract

The Perdew-Burke-Ernzerhof (PBE) generalized gradient approximation (GGA) is adopted to simulate the electronic structures and optical properties of  $\text{AgInS}_2$  semiconductors with S substitution by chalcogenides. The chalcogenide-doped  $\text{AgInS}_2$  semiconductor can be synthesized at the normal conditions due to the formation energies. O and Se doping in  $\text{AgInS}_2$  remain the semiconductor with the narrow band gaps, while Te doping converts semiconductor to metal. In the presence of the impurities, the contributions from p states of chalcogenides are involved, accountable for the reduction of the band gaps. Using the reflectivity and absorption coefficients, the optical properties with extensive absorption range and low reflectivity are attained by incorporating  $\text{AgInS}_2$  semiconductors with chalcogenides. Finally, this theoretical work launches a broader understanding of the absorber materials and also predicts the natural properties as the alternative for the solar cell applications.

# Introduction

The express development of human economy in present society has led to progressively noticeable environmental pollution and energy shortage problems. The efficient and pollution-free energy resource has become the top significance of human energy advancement in these decades. Ternary chalcogenide materials have been currently received attention from these scientific topics because of their efficient technological applications. [1–9]  $\text{AgInS}_2$  is one of the I-III-VI<sub>2</sub> ternary chalcogenide semiconductors widely used in the active fields of photovoltaic cells, photocatalysis, optoelectronics and nonlinear optics [10–13]. In addition,  $\text{AgInS}_2$  semiconductor is a suitable material to be implemented as visible light absorber layers because of its optimal band gap, high absorption coefficient and low toxicity. [14, 15] In order to improve the electronic structures and optical properties for the solar cell applications, researchers have adopted numerous routes to improve and manipulate these properties including doping. For instance, chalcopyrite  $\text{AgInS}_2$  thin films doped with Sn were synthesized by spray pyrolysis technique. [16, 17] The n-type to p-type transformation was achieved by incorporating Sn. In addition, the conduction type could be changed from n to p-type by Sb doping in  $\text{AgInS}_2$  crystals. [18]  $\text{AgInS}_2$  photoelectrode doped with Ga was prepared by a hydrothermal and electrochemical deposition approaches. [19] Ga doping in  $\text{AgInS}_2$  displayed high photocurrent density and improved the absorption range to the visible light. Cu doping in  $\text{AgInS}_2$  and  $\text{AgInS}_2/\text{ZnS}$  nanocrystals was first synthesized by a surface doping technique. [20] Cu dopant extended the photoluminescence lifetime of these nanocrystals. The synthesis of Zn-doped  $\text{AgInS}_2$  nanocrystals was achieved via a facile solution technique. [21] Using the reaction temperature, Zn doping in these nanocrystals manipulated the optical emissions into the visible light region. The experimental studies [22–24] underlined that  $\text{AgInS}_2$  doped Zn exhibited the multicolour of the visible light wave lengths because of the tunable band gap in the visible region. Using the density functional theory, the electronic structures and optical properties of  $\text{AgInS}_2$  in wurtzite phase with vacancy defects and Zn coefficients of  $\text{AgInS}_2$  were promoted when

substituted Ag and In by Zn. But so far, the origin of chalcogenides doping in AgInS<sub>2</sub> semiconductor has not been studied. Herein, it is essential to determine the electronic structures and optical properties of chalcogenide-doped AgInS<sub>2</sub> by simulated calculations to reveal their change mechanism with the purpose to guide the experiments better.

For the demonstration, the state-of-the-art density functional theory technique in the framework of the general gradient approximation (GGA) is commonly implemented by researchers because of the convenient calculation genre and lower demand of computer resource. To fill this gap, the inspiration is to profoundly determine the electronic structures and optical properties of AgInS<sub>2</sub> semiconductors doped with chalcogenides like O, Se and Te by GGA method with the Perdew-Burke-Ernzerhof correction (PBE) exchange correlation potential [26]. I hope that this work can conduct some praiseworthy theoretical guideline for the solar cell applications based on these studied materials. For the presentation, the manuscript is structured as follows. A brief description of the crystal structure and the theoretical background essential to perform the computations is delivered in Sect. 2. In Sect. 3, the results and analysis of all configurations are reported. Finally, Sect. 4 conveys the conclusions.

## Theory

To request the electronic and optical properties of doped AgInS<sub>2</sub> semiconductors, all calculations are carried out with the density function theory as implemented in Cambridge serial total energy package (CASTEP) [27, 28]. The Perdew-Burke-Ernzerhof (PBE) generalized gradient approximation (GGA) method is utilized to describe the exchange functional. The calculations adopt the unit cell of orthorhombic AgInS<sub>2</sub> with Pna2<sub>1</sub> space group which consists of 16 atoms as displayed in Fig. 1. Plane waves with kinetic energy up to 520 eV are considered in the calculations. For the sampling of the irreducible Brillouin zone, Monkhorst-Pack k-points meshes with grids of 4 × 4 × 4 are used. The optimization algorithm is selected as the Broyden-Fletcher-Goldfarb-Shanno (BFGS) scheme. [29–32] For the accurate and reliable computations, the convergence criteria is set as follows: the total energy, maximum force, maximum stress and maximum displacement are defined as 2.0×10<sup>-6</sup> eV/atom, 1.0×10<sup>-5</sup> eV/Å, 0.05 GPa and 0.001 Å, respectively. Using this computational technique, AgInS<sub>2</sub> lattice constants are a = 6.8057 Å, b = 7.1530 Å, c = 8.3536 Å. These lattice parameters agree well with the previous results {(a = 6.69 Å, b = 6.98 Å, c = 8.18 Å) [9], (a = 6.69 Å, b = 6.99 Å, c = 8.27 Å) [2], (a = 6.68 Å, b = 6.99 Å, c = 8.25 Å) [4], (a = 6.81 Å, b = 7.14 Å, c = 8.33 Å) [5]}. In addition, band gap of AgInS<sub>2</sub> with 0.964 eV is quite consistent with the available data (0.40 eV [9] and 0.65 eV [5]), while there is a large discrepancy with some literatures (1.98 eV [33], 2.08 eV [9] and 2.09 eV [5]). The calculated value is very small when compared to the experimental value (1.98 eV [33]). This is due to the fact that employing the GGA method leads to the underestimation of band gap. Owing to the obtainable comparison, this approach can be a suitable choice to study the electronic and optical properties of AgInS<sub>2</sub> semiconductor with S substitution by chalcogenide atoms like O, Se and Te. For the computed demonstration, AgInS<sub>2</sub> compounds doped with O, Se and Te are labelled as AgIn(S<sub>1-x</sub>O<sub>x</sub>), AgIn(S<sub>1-x</sub>Se<sub>x</sub>) and AgIn(S<sub>1-x</sub>Te<sub>x</sub>), respectively. To fill this gap, formation energies, band gaps,

electronic band structures, density of states, partial density of states, reflectivity and absorption coefficients are utilized to evaluate and analyzed the physical properties.

## Results And Discussions

Using GGA method with PBE exchange functional, the goal of the following is to understand how the electronic structures and optical properties of  $\text{AgInS}_2$  change after chalcogenides (O, Se and Te) doping and to predict their abilities for the competent absorber materials in the photovoltaic devices. The theoretical recommendation before the actual manufacture is imperative. The chalcogenides doping in  $\text{AgInS}_2$  material lead to the changes in the physical properties due to the alteration in crystal symmetry. First, Table I itemizes the formation energies and their band gaps at equilibrium. Due to the formation energies, the chalcogenides doping in  $\text{AgInS}_2$  semiconductor can be synthesized at the normal conditions. From the qualitative point of view,  $\text{AgIn(S, O)}_2$  is the most stable among all studied systems.  $\text{AgIn(S, O)}_2$  and  $\text{AgIn(S, Se)}_2$  remain the semiconductor with the reduced band gaps, while  $\text{AgIn(S, Te)}_2$  becomes metallic. To scrutinize the electronic properties, the electronic band structures of  $\text{AgInS}_2$  semiconductors doped with different chalcogenides are schemed in Fig. 2 along the several high symmetry lines in the irreducible Brillouin zone. As can be seen in  $\text{AgIn(S, O)}_2$  and  $\text{AgIn(S, Se)}_2$ , the conduction band minimum and the valence band maximum are both located at the  $\Gamma$  point, subsequently displaying the direct band gaps. The decreased band gaps of  $\text{AgIn(S, O)}_2$  and  $\text{AgIn(S, Se)}_2$  can be described by the fact that the conduction bands shift towards the Fermi level ( $E_F$ ). For  $\text{AgIn(S, Te)}_2$ , the Fermi level is spanning across the conduction bands, leading to the metallic behaviour. Combining this downshift of the conduction band minimum by dopants, these materials can provide an approach to optimize the band edge positions and band gaps for the solar cell applications. Through the electronic properties, these explorations are supportive for the absorption of spectra with special frequencies corresponding to their band gaps.

The composition of the calculated band structures under various doped chalcogenides is analyzed via the total and partial density of states as shown in Fig. 3. The upper valence bands of  $\text{AgInS}_2$  with the energy range 0.0 eV to -4.0 eV are mostly formed by S-p states and marginally from Ag-d and In-p states. The lower valence bands less than -4.0 eV are typically dominated by Ag-d states. Above the Fermi level, the conduction bands are mainly from the hybridization of In-p and S-p orbitals. In the energies greater than 3.0 eV, In-p states are mostly promoted in the upper conduction bands. In the presence of the impurities, the contributions of p states from chalcogenides are additionally included into both lower conduction and upper valence bands. Close examination nearby the region of the band gap demonstrates that these p states from the dopants mainly play an important role in decreasing the conduction band edge, thus yielding the reduction of the band gaps.

In addition,  $\text{AgInS}_2$  is a gorgeous semiconductor for optoelectronic and photovoltaic applications owing to its relatively great absorption coefficient and suitable energy band gap. Therefore, the optical

different chalcogenides are imperative to be

determined. The reflectivity coefficients of  $\text{AgInS}_2$  semiconductors under various dopants are plotted in Fig. 4. The static reflectivities ( $R(0)$ ) are improved in the presence of impurities. The highest value is probed in  $\text{AgIn}(\text{S}, \text{Te})_2$ . The chalcogenides doping in  $\text{AgInS}_2$  reduce the first peaks of the reflectivity curves. The maximum peaks of all compounds are positioned in the ultraviolet region. The results highlight that the reflectivity coefficients of all doped  $\text{AgInS}_2$  are reduced in the ultraviolet section compared with pure  $\text{AgInS}_2$ . To obtain more detailed optical properties, the computed absorption coefficients of  $\text{AgInS}_2$  semiconductors doped with various chalcogenides are plotted in Fig. 5. The first peaks of the absorption coefficients are located in the energy range from 0.0 to 2.0 eV because of the direct inter-band transitions from the highest valence band to the lowest conduction band. In the presence of the dopants, the red shift in the first peaks of the absorption spectra is obtained, leading to the extension of the absorption assortment. The absorption coefficients of these peaks are reduced when doping with chalcogenides. The main peaks are located in the ultraviolet area with the energy ranging from 5.0 eV to 10.0 eV. There are manifold peaks around the main peak, representing a high absorption region in the extensive energy range nearby the main peak. In addition, the absorption coefficients at these peaks have continually decreasing tendency when doping. Therefore, the optical properties with extensive absorption range and low reflectivity are carried out by doping  $\text{AgInS}_2$  semiconductors with chalcogenides. Finally, the theoretical prediction recommend that these studied materials are of prime importance for the absorber of solar cells based on chalcogenide-doped  $\text{AgInS}_2$  semiconductors.

## Conclusions

I successfully determine the electronic structures and optical properties of chalcogenide-doped  $\text{AgInS}_2$  semiconductors by the GGA method with PBE exchange functional. To sum up, the remarkable results are presented as follows:

1. **Electronic properties:** According to the formation energies, the chalcogenides doping in  $\text{AgInS}_2$  semiconductors can be synthesized at the regular conditions. The most stable material is observed in  $\text{AgIn}(\text{S}, \text{O})_2$ .  $\text{AgIn}(\text{S}, \text{O})_2$  and  $\text{AgIn}(\text{S}, \text{Se})_2$  display the semiconductor with the reduced band gaps while  $\text{AgIn}(\text{S}, \text{Te})_2$  is characterized as metal.
2. **Density of state:** The upper valence bands of  $\text{AgInS}_2$  are mostly formed by S-p states and slightly from Ag-d and In-p states. The lower valence bands are typically promoted by Ag-d states. The conduction bands are mainly from the contribution of In-p and S-p orbitals. In the presence of the dopants, the contributions of p states from chalcogenides are also included into both lower conduction and upper valence bands. The p states of the dopants principally play an important role in decreasing the conduction band edge, thus leading to the reduced band gaps.
3. **Optical properties:** The reflectivity coefficients are condensed by the impurities. In the presence of the dopants, the red shift of the absorption coefficients is attained, thus leading to the expansion of the absorption range. The optical properties with wide absorption variety and low reflectivity are achieved by doping  $\text{AgInS}_2$  semiconductors with the impurities.

Finally, it is expected that these theoretical investigations deliver a detailed understanding to enlighten the enhancement of the photovoltaic performance in the solar cell applications based on doped AgInS<sub>2</sub> semiconductors.

## Declarations

### Acknowledge

The author would like to acknowledge the support from Department of Physics, Faculty of Science, Ubon Ratchathani University, Thailand.

## References

- [1] J. E. Jaffe, A. Zunger, Phys. Rev. B 29 (1984) 1882.
- [2] G. Delgado, A. J. Mora, C. Pineda, T. Tinoco, Mater. Res. Bull. 36 (2001) 2507.
- [3] A. A. Vaipolin, Yu. V. Rud, I. V. Rozhdestvenskaya, Cryst. Res. Technol. 23 (1988) 337.
- [4] J. Krustok, J. Raudoja, M. Krunks, H. Mandar, H. Collan, J. Appl. Phys. 88 (2000) 205.
- [5] J. Liu, S. Chen, Q. Liu, Y. Zhu, Y. Lu, Comp. Mater. Sci. 91 (2014) 159.
- [6] S. Sharma, A. S. Verma, V. K. Jindal, Physica B 438 (2014) 97.
- [7] A. S. Verma, S. R. Bhardwaj, J. Phys.: Condens. Matter 19 (2007) 026213.
- [8] V. Jayalakshmi, S. Davapriya, R. Murugan, B. Palanivel, J. Phys. Chem. Solids 67 (2006) 669.
- [9] G. M. Dongho Nguimdo, D. P. Joubert, Eur. Phys. J. B 88 (2015) 113.
- [10] K. P. Kadlag, M. J. Rao, A. Nag, J. Phys. Chem. Lett. 4 (2013) 1676.
- [11] T. Torimoto, M. Tada, M. Dai, T. Kameyama, S. Suzuki, S. Kuwabata, J. Phys. Chem. C 116 (2012) 21895.
- [12] M. Deng, S. Shen, X. Wang, Y. Zhang, H. Xu, T. Zhang, Q. Wang, Cryst Eng Comm 15 (2013) 6443.
- [13] D. Gherouel, I. Gaied, M. Amlouk, J. Alloy. Compd. 566 (2013) 147.
- [14] J. Han, Z. Liu, K. Guo, J. Ya, Y. Zhao, X. Zhang, T. Hong, J. Liu, ACS Appl. Mater. Interfaces 6 (2014) 17119.
- [15] C. A. Arredondo, J. Clavijo, G. Gordillo, J. Phys.: Conf. Ser. 167 (2009) 012050.

- [16] M. L. Albor Aguilera, J. R. Aguilar Hernández, M. A. González Trujillo, M. Ortega Lopez, *Solar Energy Materials and Solar Cells* 91 (2007) 1483.,
- [17] M. L. Albor-Aguilera, D. Ramírez-Rosales, M. A. González-Trujillo, *Thin Solid Films* 517 (2009) 2535.
- [18] K. Yoshino, H. Komaki, T. Kakeno, Y. Akaki, T. Ikari, *Journal of Physics and Chemistry of Solids* 64 (2003) 1839.
- [19] Qijun Cai, Zhifeng Liu, Junwei Li, Changcun Han, Zhengfu Tong, *Catalysis Letters* volume 150 (2020) 1089.
- [20] Siqi Chen, Violeta Demillo, Minggen Lu and Xiaoshan Zhu, *RSC Adv.* 6 (2016) 51161.
- [21] Xiaosheng Tang, Wenxi Bernice Ailsa Ho and Jun Min Xue, *J. Phys. Chem. C* 116 (2012) 9769.
- [22] T. Torimoto, T. Adachi, K. Okazaki, M. Sakuraoka, T. Shibayama, B. Ohtani, A. Kudo, S. Kuwabata, *J. Am. Chem. Soc.* 129 (2007) 12388.
- [23] X. Tang, W.B.A. Ho, J.M. Xue, *J. Phys. Chem. C* 116 (2012) 9769.
- [24] Y. Hamanaka, T. Ogawa, M. Tsuzuki, T. Kuzuya, *J. Phys. Chem. C* 115 (2011) 1786.
- [25] Jianbo Yin, Xuefeng Lu, Qizheng Dong, *Computational Materials Science* 122 (2016) 86.
- [26] J. P. Perdew, K. Ernzerhof, M. Burke, *Phys. Rev. Lett.* 77 (18) (1996) 3865.
- [27] S. J. Clark, M. D. Segall, C. J. Pickard, P. J. Hasnip, M. J. Probert, K. Refson, M. C. Payne *Zeitschrift für Kristallographie* 220 (5-6) (2005) 567.
- [28] M. D. Segall, P. J. D. Lindan, M. J. Probert, C. J. Pickard, P. J. Hasnip, S. J. Clark, M. C. Payne, *J. Phys.: Condens. Matter* 14 (11) (2002) 2717.
- [29] C. G. Broyden, *J. Inst. Math. Appl.* 6 (1970) 76.
- [30] R. Fletcher, *Computer J.* 13 (1970) 317.
- [31] D. Goldfarb, *Math. Comput.* 24 (1970) 23.
- [32] D. F. Shanno, *Math. Comput.* 24 (1970) 647.
- [33] D. Huang, C. Persson, *Chem. Phys. Lett.* 591 (2014) 189

## Tables

Table I: The calculated formation energies and band gaps of  $\text{AgInS}_2$  materials with S substitution by O,

Loading [MathJax]/jax/output/CommonHTML/fonts/TeX/fontdata.js

	$\text{AgInS}_2$	$\text{AgIn(S, O)}_2$	$\text{AgIn(S, Se)}_2$	$\text{AgIn(S, Te)}_2$
Formation energies (eV)	-	-7.232	-0.442	-1.027
Band gap (eV)	0.964	0.059	0.265	0.000

## Figures

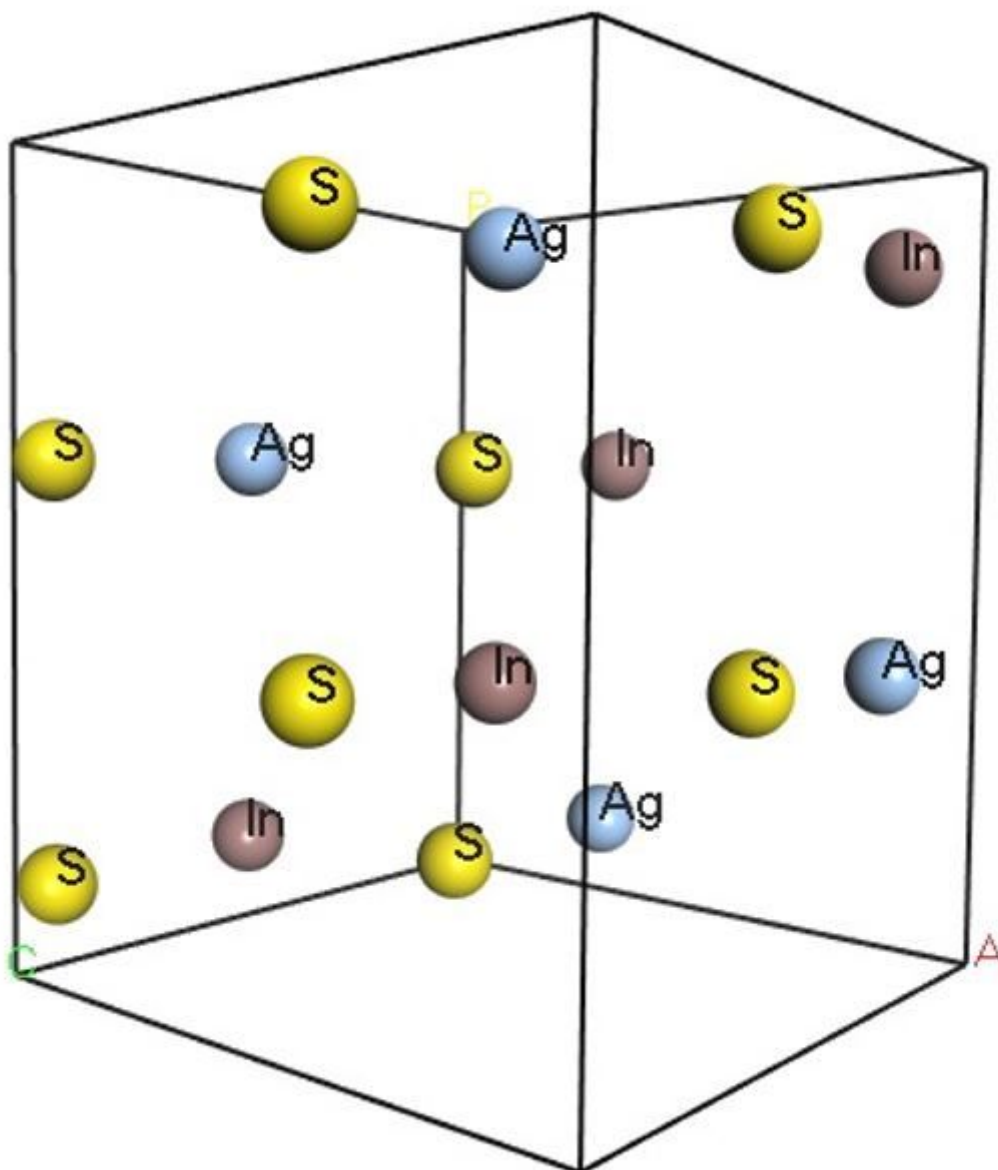
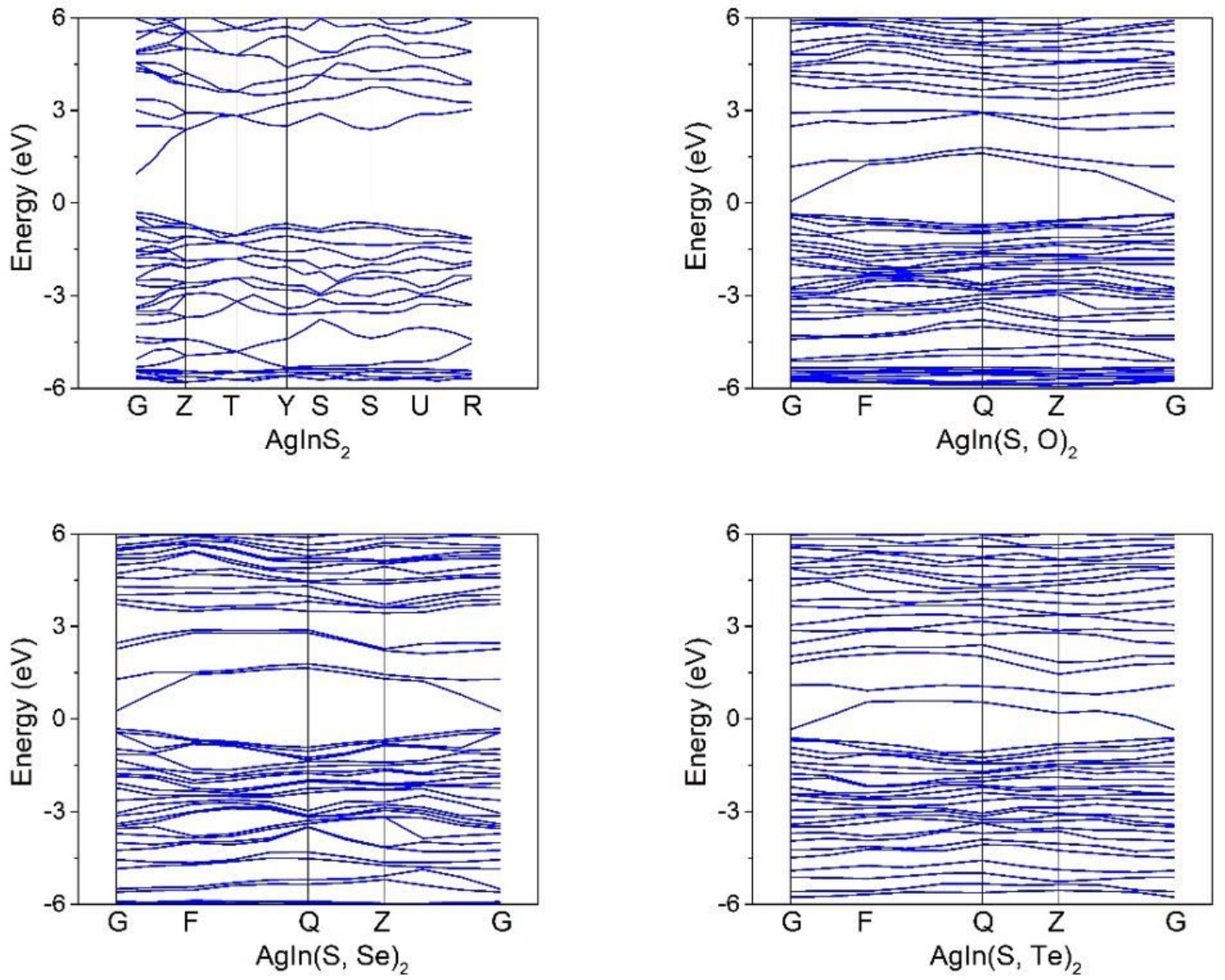


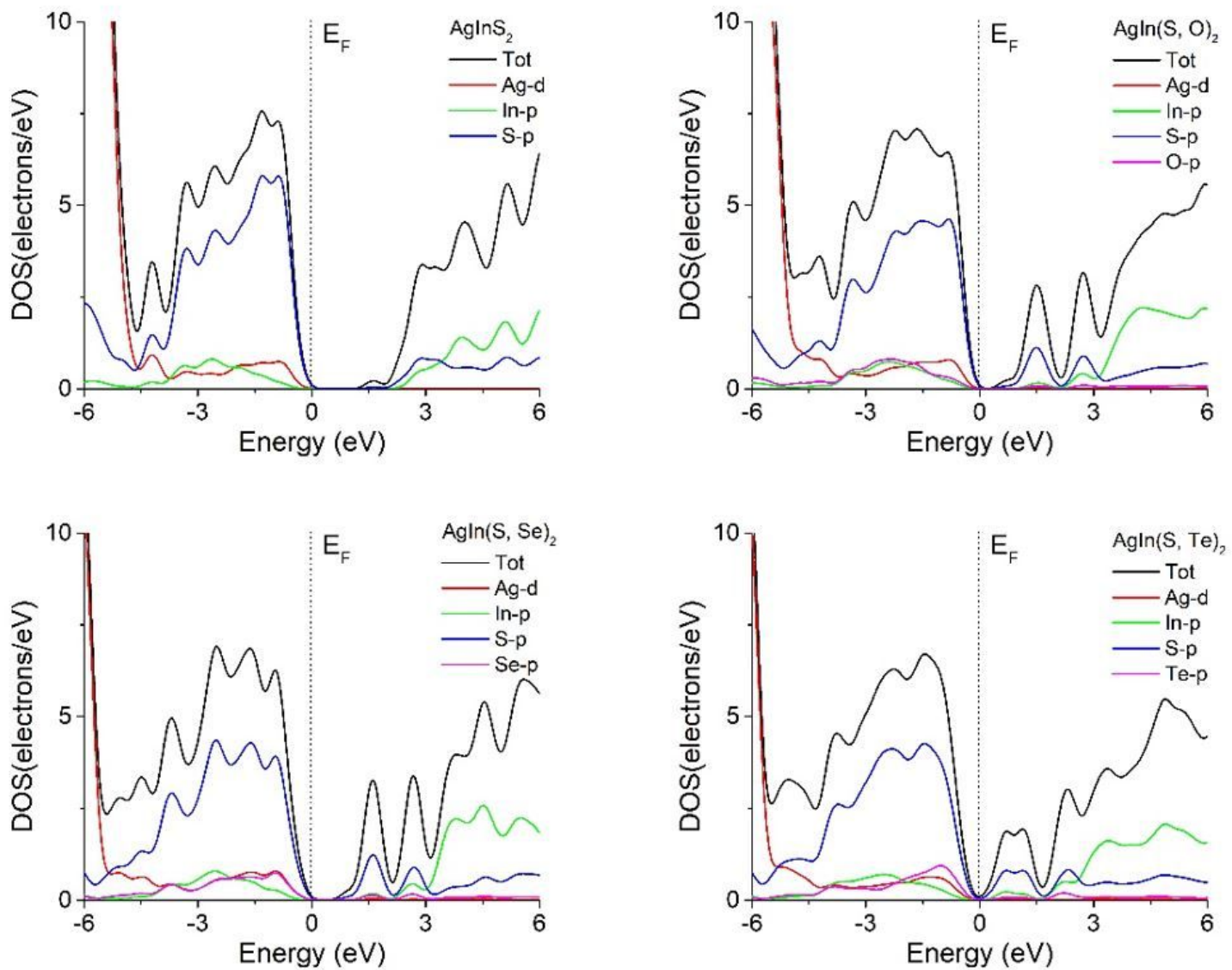
Figure 1

Illustration of  $\text{AgInS}_2$  semiconductor.



**Figure 2**

Band structures of  $\text{AgInS}_2$ ,  $\text{AgIn(S, O)}_2$ ,  $\text{AgIn(S, Se)}_2$  and  $\text{AgIn(S, Te)}_2$  material.



**Figure 3**

The total and partial density of states of  $\text{AgInS}_2$ ,  $\text{AgIn(S, O)}_2$ ,  $\text{AgIn(S, Se)}_2$  and  $\text{AgIn(S, Te)}_2$  material.

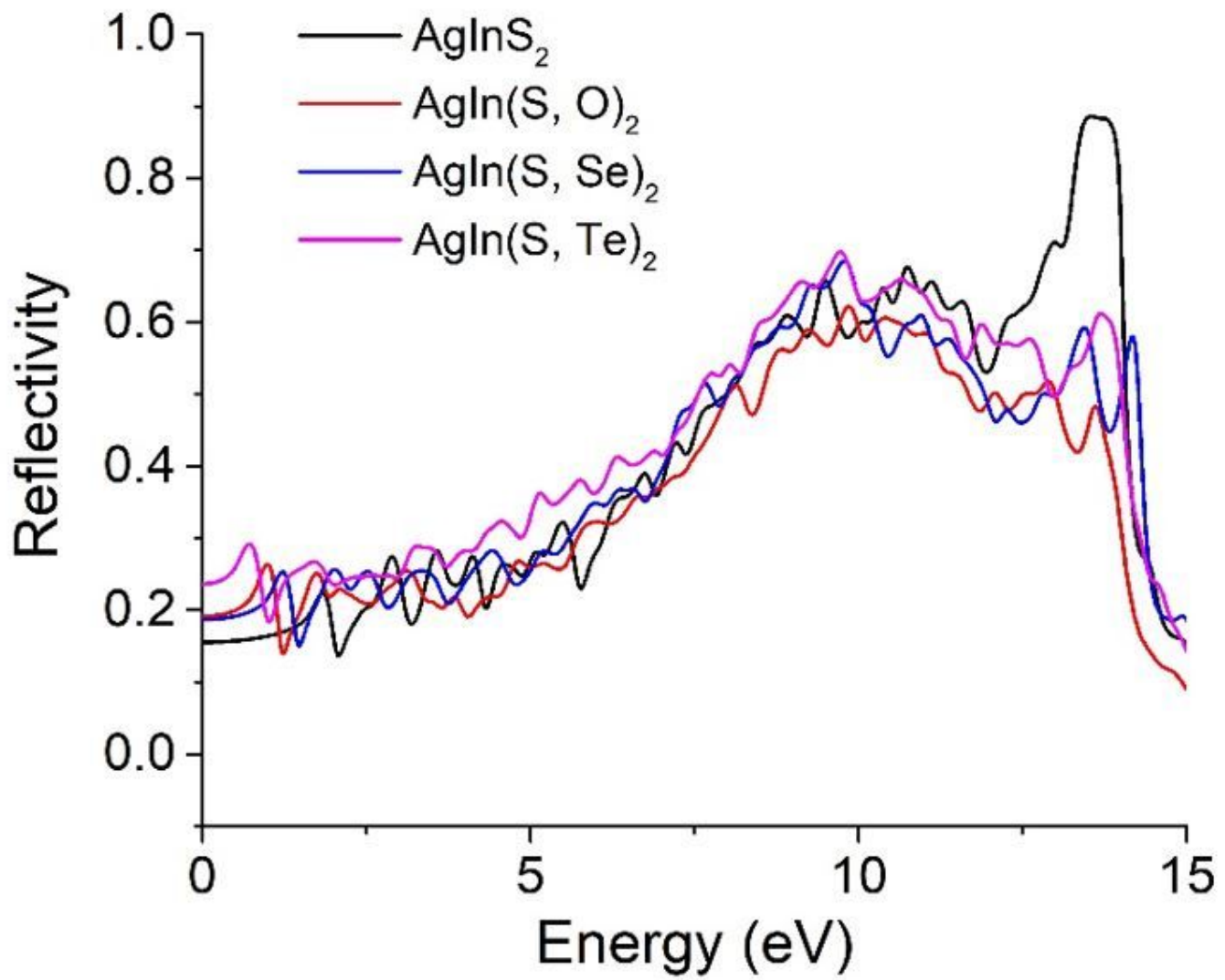


Figure 4

Optical reflectivity coefficients of AgInS<sub>2</sub>, AgIn(S, O)<sub>2</sub>, AgIn(S, Se)<sub>2</sub> and AgIn(S, Te)<sub>2</sub> material.

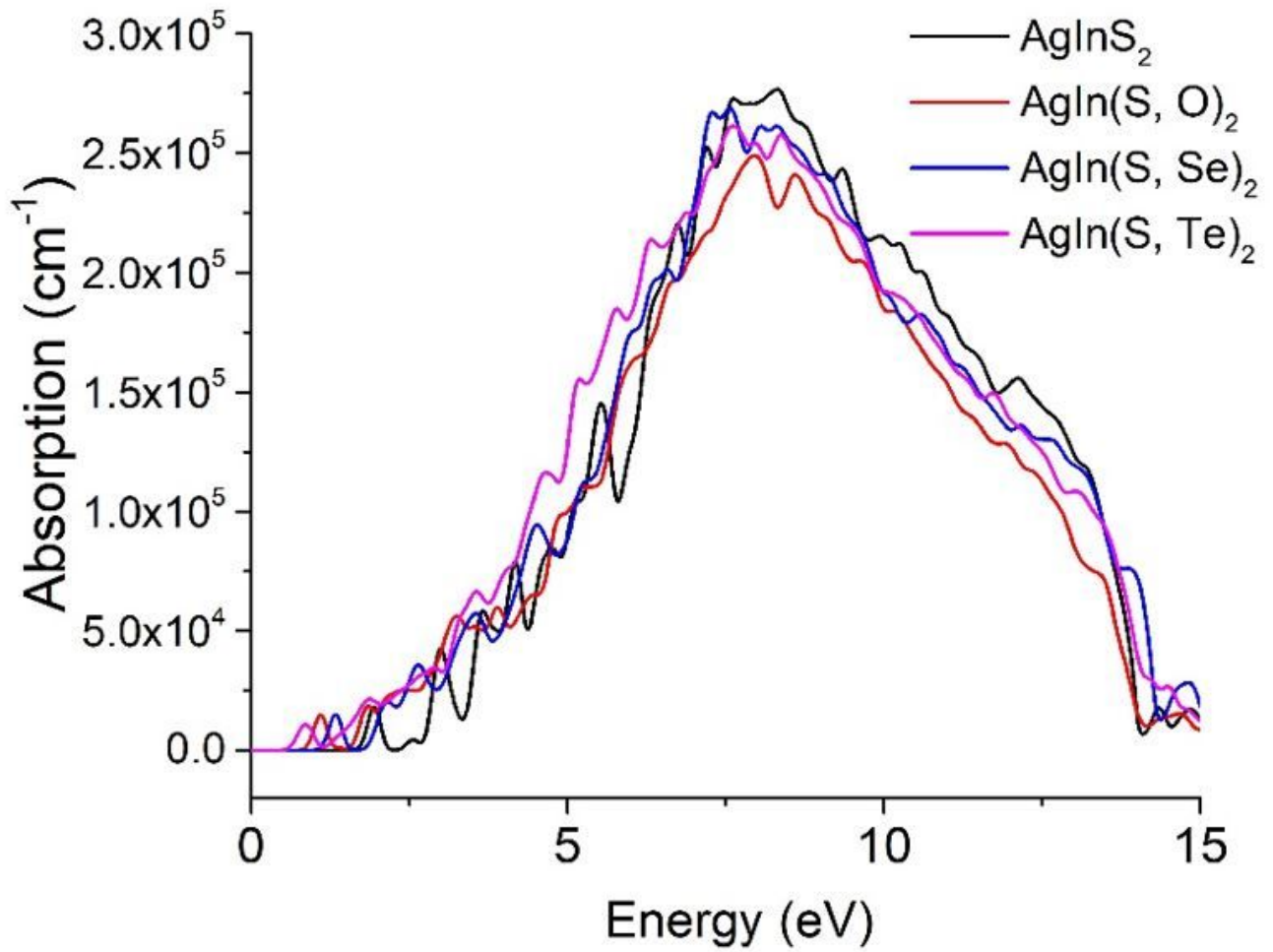


Figure 5

Absorption spectra of AgInS<sub>2</sub>, AgIn(S, O)<sub>2</sub>, AgIn(S, Se)<sub>2</sub> and AgIn(S, Te)<sub>2</sub> material.